JOURNAL OF NEUROTRAUMA 31:1881–1895 (November 15, 2014)

DOI: 10.1089/neu.2014.3343

The Acute Phase of Mild Traumatic Brain Injury Is Characterized by a Distance-Dependent Neuronal Hypoactivity

Victoria P.A. Johnstone,[1] Sandy R. Shultz,[2] Edwin B. Yan,[1] Terence J. O'Brien,[2] and Ramesh Rajan[1]

Abstract

The consequences of mild traumatic brain injury (TBI) on neuronal functionality are only now being elucidated. We have now examined the changes in sensory encoding in the whisker-recipient barrel cortex and the brain tissue damage in the acute phase (24 h) after induction of TBI ($n = 9$), with sham controls receiving surgery only ($n = 5$). Injury was induced using the lateral fluid percussion injury method, which causes a mixture of focal and diffuse brain injury. Both population and single cell neuronal responses evoked by both simple and complex whisker stimuli revealed a suppression of activity that decreased with distance from the locus of injury both within a hemisphere and across hemispheres, with a greater extent of hypoactivity in ipsilateral barrel cortex compared with contralateral cortex. This was coupled with an increase in spontaneous output in Layer 5a, but only ipsilateral to the injury site. There was also disruption of axonal integrity in various regions in the ipsilateral but not contralateral hemisphere. These results complement our previous findings after mild diffuse-only TBI induced by the weight-drop impact acceleration method where, in the same acute post-injury phase, we found a similar depth-dependent hypoactivity in sensory cortex. This suggests a common sequelae of events in both diffuse TBI and mixed focal/diffuse TBI in the immediate post-injury period that then evolve over time to produce different long-term functional outcomes.

Key words: barrel cortex; electrophysiology; hypoexcitability; mild TBI; neuronal encoding; sensory cortex

Introduction

Traumatic brain injury (TBI), as occurs in falls, vehicle collisions, and sporting and military accidents, is a major global public health concern, with more than 57 million people worldwide having been hospitalized with one or more incidences of TBIs.[1] Most injuries are relatively mild in nature, and patients present with a complex combination of focal and diffuse injury. Focal injury is produced by collision forces acting on the skull and resulting in local tissue compression beneath the site of impact.[2] Such injuries are commonly characterized by laceration, contusion, and hematoma occurring in either the presence or absence of a skull fracture.[3] In contrast, diffuse brain injury occurs from rapid acceleration-deceleration of the head (as seen, for example, in high-speed motor vehicle accidents[4,5]) and involves diffuse axonal and vascular injury, brain swelling, and hypoxic ischemic damage.[6]

The processes leading to injury can be classified as primary and secondary injury mechanisms.[7–11] Primary mechanisms are attributed to mechanical events during impact with the brain and include brain contusion, hematomas, hemorrhage, and axonal disruption.[11–13] These events are followed by secondary injury processes that manifest over hours to days[14] and involve dynamic cascades that induce ionic imbalances, excitotoxicity, oxidative stress, hypoxia-ischemia, inflammation, and cerebral edema.[8,9,11,15] For patients who survive the primary insults, mortality and functional outcomes are compounded by the secondary injury processes and the extent of their progression.[10]

Very little is known about how the primary and secondary injury processes (and their interactions) affect the neuronal responses that underlie behavior.[16] We have recently produced a comprehensive set of studies[17–19] that report dynamic changes in neuronal responses after diffuse injury using the weight-drop impact acceleration (WDIA) model.[9,20] We found, at 24 h post-injury,[18,19] a depth-dependent suppression of cortical population neuronal responsiveness for both mild and severe diffuse injury, with degree of suppression being graded to injury severity. This initial hypoactivity developed into supragranular hyperexcitability combined with normal responses in granular and infragranular layers by 8 weeks post-injury.[17]

Although the early time point is likely to involve primary and secondary injury mechanisms[9,10,14] while the later time point will involve only secondary mechanisms, the marked difference in neurophysiological and behavioral outcomes at the two time points

[1]Department of Physiology, Monash University, Clayton, Victoria, Australia.
[2]Department of Medicine, The Royal Melbourne Hospital, The Melbourne Brain Centre, The University of Melbourne, Parkville, Victoria, Australia.

suggests that primary and secondary diffuse TBI injury mechanisms produce substantially different changes in neuronal responses in keeping with the different mechanisms or processes they engage. Given that these neuronal responses underpin neurological outcomes, this means different neuronal response changes underlie short-term and long-term morbidity in TBI.

We now examine how mild TBI in a mixed injury model involving diffuse and focal injury affects cortical neuronal responsiveness immediately post-injury, using the lateral fluid percussion injury (LFPI) model.[9,21,22] This model causes a substantially different injury phenotype from the diffuse injury-only model we have used previously, with more persistent long-term deficits in motor coordination and, in a proportion of animals, post-traumatic seizures.[22–24] Despite these differences in long-term outcomes, we report that the acute post-injury effects are very similar in this model as in the diffuse-only model we studied previously.[18,19] This is consistent with the notion of primary injury being because of similar mechanical events during brain impact and that this is similar between different injury models. It is likely then that any differences in long-term outcome between the two models of TBI are a result of divergence in secondary injury cascades, with certain pathways exerting more or less dominance on the neuronal response, depending on the mode of injury. Development of effective therapies will therefore need to recognize a decoupling between similar primary mechanisms and subsequent secondary mechanisms as a function of injury event.

Methods

Animals

Subjects were male Sprague-Dawley rats (8–12 weeks old) obtained from the Animal Resources Centre (Western Australia). Rats were housed individually under a 12 h light/dark cycle with food and water *ad libitum.* Each animal was randomly allocated to receive either a mild LFPI ($n = 9$) or a sham-injury ($n = 5$) treatment, and given 24 h post-injury to recover before electrophysiological testing. Experiments were performed in accordance with the National Health and Medical Research Council guidelines for the care and welfare of experimental animals, and received approval from the Monash University Standing Committee on Ethics in Animal Experimentation and the Melbourne Health Animal Ethics Committees.

LFPI

Injury procedures were based on a standard protocol as described previously and used by our group.[25–28] Briefly, anesthesia was induced with 4% isofluorane in oxygen (2 L/min) via inhalation, and maintained throughout surgery with 2% isofluorane and 500 mL/min oxygen flow delivered through a nose cone. Under aseptic conditions, rats underwent craniotomy to create a circular window (5 mm diameter) centered at A/P −3.0 mm, M/L 4.0 mm with reference to bregma to expose the dura mater. A modified female Luer-Lock cap was secured over the craniotomy window by cyanoacrylate and dental acrylic, the cap was filled with sterile fluid, and the rat was removed from anesthesia and attached to the fluid percussion device via the female Luer-Lock cap. Once the rat responded to a toe pinch, a mild fluid percussion pulse (1.0–1.5 atmospheres) was delivered by the fluid percussion device to the intact dura, to produce a mild TBI.[28–30]

Sham-injury rats underwent the same procedures except that no fluid percussion force was delivered. Immediately after the injury, the female Luer-Lock cap was removed, the scalp was sutured, and acute post-injury measures consisting of duration of apnea, duration of unconsciousness, and latency to occurrence of the self-righting reflex were monitored.[27–30] All rats were treated with analgesic (carprofen, 5 mg/kg).

Electrophysiology

At 24 h post-surgery, electrophysiological recordings from posteromedial barrel subfield (PMBSF; barrel cortex) were obtained using methods previously established in our group,[17,31,32] at both ipsilateral and contralateral locations relative to the site of injury. Animals were anesthetized using 5% halothane and tracheotomized to maintain anesthesia at 0.5–3.0% halothane through continuous ventilation. Depth of anesthesia was regularly monitored using electrocardiographic/electromyographic recordings from forepaw musculature, pinch withdrawal reflexes, and palpebral reflexes. Body temperature was maintained between 37°C and 38°C.

The skull was exposed to anchor a head bar with a screw and dental cement to the bone rostral of bregma, to hold the head firmly in place for recording. A craniotomy over the barrel cortex (either ipsilateral or contralateral to injury; approximately 4 mm diameter, centered approximately A/P −2 mm to bregma; M/L 6 mm) was made via drilling, and the exposed barrel cortex (with dura intact) was penetrated with a tungsten microelectrode (2–4 MOhm; FHC) using a fast-stepping microdrive (Kopf Model 2660) mounted on a complex of translators and goniometers.[31,32] Advancement of the electrode was monitored via high-power microscopy, by monitoring electrode depth on the calibrated microdrive, and by monitoring the amplified and filtered electrode output through speakers and on an oscilloscope.

The microdrive was zeroed at the cortical surface under high-power microscopy and then used to advance the electrode to a depth between 600 and 800 μm from the cortical surface for accurate determination of the Principal Whisker (PW; the whisker providing main excitatory input) via manual whisker deflection, using methods and criteria as described previously.[31,32] After unequivocal determination of the PW, the electrode was retracted to the surface, rezeroed again under high-powered microscopy, and then advanced systematically in 10-μm steps to record from the various cortical laminae, while monitoring depth on the microdrive.

Recording site was not altered once a PW had been obtained, because deflection of the PW invariably produced finely tuned responses in L4/L5, regardless of which whisker was the PW. Recording locus was largely determined by proximity to blood vessels and physical accessibility of the recording apparatus. Septal regions were avoided and easily demarcated on the basis of multiwhisker evoked responses that were weakly driven and tended to be more rapidly adapting.

Output signals from the electrode were amplified and band-pass filtered from 0.3–10 kHz.[31,32] On-line displays of rasters of spike occurrences and peristimulus time histograms (PSTHs) were generated using Spike2 software. A copy of the filtered neural signal was also recorded by Spike2 to allow for offline extraction of single neuron data from the cluster population responses.

Controlled whisker deflections

The methods for applying motion patterns to the PW have been detailed previously.[31] The PW was threaded through a hole on a motor-controlled level arm system positioned 5 mm from the face. The lever arm was moved under computer control in well-defined motion patterns while neural recordings were obtained from the barrel cortex. We used a range of simple and complex whisker stimuli, as we have found previously that differing complexity of afferent input is an important variable capable of highlighting changes in post-injury cortical processing.[17] A suite of five trapezoidal stimuli was initially used to characterize basic cluster responses in lamina and to extract single unit waveforms. Only the onset ramp velocity varied with these stimuli (30, 60, 150, 250, or

400 mm/sec), with deflection amplitude fixed at 3.6 mm, the trapezoid hold duration kept constant at 20 msec, and the offset ramp duration fixed at 40 msec. The suite of five stimuli was repeated 100–150 times, with each repetition consisting of the five stimuli presented pseudorandomly. The number of repetitions of each stimulus was chosen to ensure that there were enough waveforms obtained for reliable spike sorting.

Standard Spike2 template matching algorithms were applied to generate individual spike waveform templates from the responses, and in most cases, 3–4 waveforms were obtained at any recording location. These templates were applied at that recording point to separate responses of different presumptive neurons to the trapezoid stimuli and the subsequent complex whisker motion stimuli (see below), for later off-line analysis.

Two complex ''naturalistic'' whisker deflections were then applied in turn to the PW, one modeling the whisker motion videographed in rats making contact with a rod placed in the path of the whiskers and then moving the whiskers past the rod,[33] and the other modeling the whisker motion across rough surfaces exhibited by rats trained to discriminate between rough and smooth surfaces.[34] The use of both sets of complex stimuli was important to ascertain whether different neuronal output could be detected depending on the nature of the complex afferent sensory information used to evoke responses.

The methods for extracting these stimuli from the original reports[33,34] and storing and playing them out from text files have been detailed previously.[17] Ten stimulus amplitudes were used for each of the two complex whisker motions, beginning with an amplitude of 0.2 mm and then continuing from 0.4–3.6 mm, in 0.4-mm steps. Each stimulus amplitude was presented 50 times in a pseudorandom order.

Data analysis

As in our recent studies, clusters and single neurons were collated into laminae by depth as Layer 2 (150–300 μm from the cortical surface); Upper Layer 3 (350–500 μm); Deep Layer 3 (550–700 μm); Layer 4 (750–1000 μm); and Layer 5 (1100–1400 μm). All neuronal recordings are shown as firing rate (Hz) in 1 msec bins over the period from 200 msec before stimulus onset until 100 msec post-stimulus offset. The data from the clusters was used for off-line analysis to generate population PSTHs; PSTHs for all neuronal clusters in a lamina were averaged to produce a laminar Grand PSTH to show the pattern of population responses within a lamina. A responsive unit was defined as one with responses significantly greater than spontaneous rate over at least three successive stimulus amplitudes (naturalistic stimuli)/velocities (trapezoids).

The PSTHs were generated by averaging responses to each stimulus amplitude (for the complex stimulus waveforms) or each stimulus ramp velocity (for the trapezoid stimuli) across all presentations of that stimulus. The averages were corrected for spontaneous firing rate, using the 200 msec pre-stimulus firing rate. Then a five-point weighted moving average was applied to smooth out any noise in the responses, and the data averaged across all multiunits to produce a Grand PSTH.

While the Grand PSTH was used to visualize the overall pattern of responses in a lamina to a stimulus, neuronal response metrics were derived separately from each cluster and single cell within a lamina. Thus, the peak firing rate, excitatory area under the curve, latency to peak firing rate, and half-peak width were calculated for clusters and single cells for each stimulus. For the trapezoidal whisker motion stimuli, these metrics were calculated separately for each trapezoid defined by a particular onset ramp velocity, and for the complex whisker motion stimuli, these metrics were calculated separately for each stimulus amplitude. For the short duration trapezoidal stimulus and the complex object contact stimulus, a 5–50 msec window after stimulus onset was used; for the longer rough texture discrimination stimuli, a 5–30 msec counting window was used. These counting windows were set to encompass the maximum response over the stimulus presentation period. Two-way repeated measures analysis of variance (ANOVA) were used for all data comparisons.

Immunohistochemistry

After electrophysiology recording, the animal was overdosed with sodium pentobarbitone (Lethobarb; 300 mg/mL), perfused transcardially first with ice-cold saline to remove blood and then fixed with 4% paraformaldehyde. The brain was removed from the cranium and post-fixed in paraformaldehyde for 24 h before processing for paraffin embedding. Then 10-μm thick sections were obtained from a region of approximately 1.3 mm caudal to bregma and processed for neurofilament heavy chain (NF-200) immunohistochemical staining using techniques described previously.[19] Monoclonal NF-H antibody (1:1000; Invitrogen) was used in conjunction with the peroxidase-diaminobenzidine method to visualize injured axons. Stained sections were scanned by ScanScope AT Turbo slide scanner (Aperio, CA) and visualized and analyzed by Aperio ImageScope (v11.2.0.780, Aperio, CA) and ImageJ (NIH).

Scanned tissue sections were viewed using Aperio ImageScope, and the perimeter of the region to be examined was defined. For cortex, this constituted a region beginning from the midline and following the border of the cingulum and the external capsule to the level of the rhinal fissure. The cingulum and external capsule were also analyzed separately. For each region of interest (ROI), multiple photos were obtained at 15x magnification to cover the entire region without overlapping. Within each ROI, automated densimetric analysis was used to calculate the total area stained for NF-200 (cell body, axons, dendrites) as a percentage of the total area within the ROI. The analysis was conducted using ImageJ. The data were analyzed by Mann Whitney *U* test between treatment groups; each region of interest was treated independently. Data are presented as mean ± standard error of the mean (SEM).

Results

Acute injury severity measures

The severity of acute injury after the fluid percussion insult was indexed in three outcomes: duration of loss of consciousness, duration of apnea, and time taken for recovery of the self-righting reflex. There was no loss of consciousness or apnea in either group of animals. There was a significant difference in time taken for recovery of the self-righting reflex, with sham animals taking 152 ± 27 sec (mean ± SEM) and mild LFPI animals taking 241 ± 8 sec ($t_{1\text{-}t} = -3.9$, $p < 0.005$). These data indicate, consistent with the LFPI parameters, that only mild TBI was caused.

Multiunit cluster responses to simple and complex whisker stimuli post-mild LFPI-induced TBI

Twenty-four hours post-injury, neuronal responses were obtained from both groups of animals from the barrel cortex in the hemisphere ipsilateral and the hemisphere contralateral to injury/sham treatment site. In all cases, responses were obtained to stimulation of whiskers in the whisker pad contralateral to the recording site. We used a variety of whisker motion patterns to elicit neuronal responses. We have previously demonstrated that the cortical hypoactivity that occurs in the acute phase after diffuse TBI occurs regardless of stimulus complexity, whereas by 8 weeks after injury, neuronal hyperexcitability is elicited predominantly by complex afferent information only, and weakly at all by simple whisker movements.[17] It was therefore critical for our current purposes to ascertain whether the complexity of incoming

information had an impact on changes in cortical processing after a mixed focal/diffuse injury. To establish this, we used one simple whisker motion and two complex whisker motions (all stimuli used in our long-term TBI study with the WDIA model) to evoke neuronal responses.

Neuronal responsiveness to whisker protraction velocity (a critical factor in evoking barrel cortex responses[31,35–37]) was assessed using simple trapezoidal patterns of whisker motion with five different onset ramp velocities from 30–400 mm/sec. Recordings were obtained from 40 responsive multiunits in barrel cortex ipsilateral to the mild LFPI, 35 responsive multi-unit clusters in barrel cortex contralateral to the mild LFPI, and 47 responsive multi-units barrel cortex in sham surgery controls.

The Grand PSTHs obtained at the highest ramp velocity (400 mm/sec) in the five laminae in the barrel cortices on the two sides relative to the injury side in mild LFPI animals and in sham surgery controls are compared in Figure 1A. In sham surgery controls (left column, Fig. 1A) in all layers, the population response consisted of a single peak during stimulus onset, followed by low levels of tonic excitation during the trapezoid hold phase, and then a second peak corresponding to stimulus offset. In marked contrast, in barrel cortex ipsilateral to the mild LFPI (right column, Fig 1A), the stimulus onset response was highly suppressed in all cortical laminae, with a concurrent absence of the offset response in Layer 2, Upper Layer 3, and Deep Layer 3, and a very weak offset response in Layers 4 and 5. Response suppression was also observed in the barrel cortex contralateral to the mild LFPI but only in the three supra-granular layers where the suppression was less striking than in the ipsilateral barrel cortex; in Layers 4 and 5, responses appeared normal. An offset peak was present in the contralateral barrel cortex, but with substantially reduced levels of tonic excitation in the preceding hold phase of the stimulus.

To quantify the changes in peak firing rate of the multi-unit clusters, response metrics were extracted using an analysis window of 5-50ms (grey shaded box in all panels of Fig. 1A) from stimulus onset and are shown in Figure 1B. Compared with sham surgery controls, peak firing rate in barrel cortex ipsilateral to the mild LFPI was significantly reduced in all layers except Layer 5 (two-way ANOVA, $p < 0.05$). There was no significant difference between peak firing rates at any velocity in any layer in the contralateral barrel cortex compared with sham controls. Although we performed two-way repeated measures ANOVAs on all groups reported here, because of the complex nature of the dataset, we include details of ipsilateral versus sham and contralateral versus sham comparisons only.

The object contact stimulus waveform, modeling the complex whisker motion of a rat brushing its whiskers past a metal post to obtain a liquid reward,[33] was applied at 10 amplitudes from 0.2–3.6 mm. Recordings were obtained from a total of 40 responsive multiunits in barrel cortex ipsilateral to the mild LFPI, 35

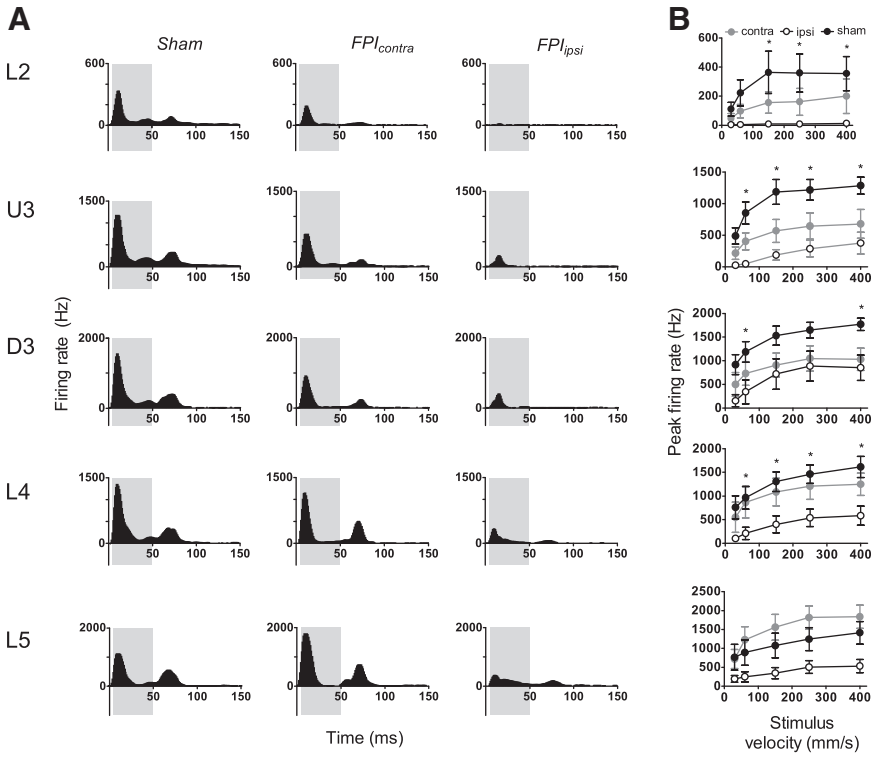

FIG. 1. Mild lateral fluid percussion injury (LFPI) effects on pattern and strength of multiunit cluster responses evoked by simple trapezoidal stimuli. Population peristimulus time histograms are shown in (**A**) in response to the trapezoid with the fastest ramp velocity (400 mm/sec) in the various lamina (indicated to the left of the panel). Recordings are from sham surgery animals and from locations contralateral (contra) and ipsilateral (ipsi) to the LFPI site. Each Grand peristimulus time histogram was generated by averaging responses across all responsive clusters within that lamina. The grey-shaded box represents the analysis window used to extract response metrics. (**B**) Peak firing rate extracted from the onset response to simple trapezoidal stimuli from clusters ipsilateral to the site of injury (white circles), contralateral to the site of injury (grey circles), and in sham animals (black circles). Data represent averages from all responsive clusters (± standard error of the mean) at all tested ramp velocities, separated by cortical lamina. Each row of data comes from the same lamina as designated by the labels on the left (* = ipsilateral vs. sham; $p < 0.05$).

responsive multiunit clusters in barrel cortex contralateral to the mild LFPI, and 50 responsive multiunits in sham surgery controls.

As for the simple trapezoid stimuli, neuronal firing was substantially dampened in response to this pattern of whisker motion in animals subjected to mild LFPI (Fig. 2A middle and right columns compared with first column). In sham surgery controls (Fig. 2A first column), the population response consisted of a large response peak after stimulus onset and a strong stimulus offset response. Grand PSTHs generated from responses in the hemisphere ipsilateral to the mild LFPI (Fig. 2A, right column) revealed very strong response suppression, particularly to stimulus onset but generally across all response components seen in the sham surgery controls. Again, this suppression showed a depth-dependency, being near-total in Layer 2 and less so with depth through Upper 3, Deep 3, Layer 4, and Layer 5, although there was clear onset response suppression all the way to Layer 5. In contrast, in the hemisphere contralateral to the mild LFPI (Fig. 2A, middle column) both onset and offset peak components were evident (Fig. 2A, middle column compared with first column), and there appeared to be a small suppression only in the upper two layers.

Quantification of the peak firing rate was again performed using an analysis window of 5–50 msec (grey-shaded box, Fig. 2A) to capture the onset response. Analysis showed a significant depression of firing rate in ipsilateral barrel cortex compared with sham surgery controls in all cortical layers except Layer 5 (Fig. 2B; two-way ANOVA, $p < 0.05$). There was no significant difference between peak firing rates in any layer in the contralateral barrel cortex compared with sham controls.

The complex rough surface discrimination waveform, modeling whisker motion of a rat trained to discriminate texture as it brushed its whiskers along a rough surface,[34] was applied at 10 amplitudes from 0.2–3.6 mm. Recordings were obtained from a total of 44 responsive multiunits in barrel cortex ipsilateral to the mild LFPI, 36 responsive multi-unit clusters in barrel cortex contralateral to the mild LFPI insult, and 47 responsive multiunits in sham surgery controls.

The Grand PSTHs generated from responsive multiunit clusters in sham surgery controls to this stimulus exhibited a single onset peak in all layers, which was followed by a small slow offset component that was clearly evident (Fig. 3A, left column). In mild LFPI animals, the onset peak was substantially reduced in all layers in barrel cortex ipsilateral to the mild LFPI, again demonstrating a depth dependency to the suppression, and in Layer 4 was divided into two or more peak components. Peak amplitude was also reduced in the contralateral hemisphere, although to a much lesser extent, and only in Layers 2 and 3.

A narrower analysis window of 5–30 msec was used to quantify the peak firing rate to stimulus onset from these responses (grey-shaded box, Fig. 3A) to encompass the entire stimulus period. These data are shown in Figure 3B and generally confirmed the

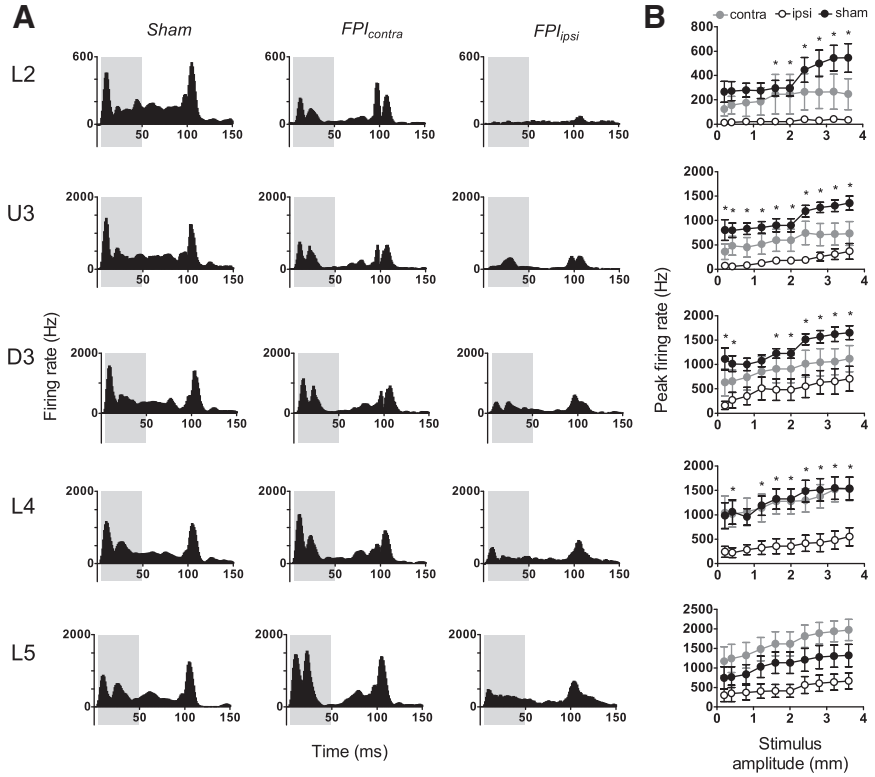

FIG. 2. Mild lateral fluid percussion injury (LFPI) effects on pattern and strength of multiunit cluster responses evoked by complex object contact stimuli. Population peristimulus time histograms are shown in (**A**) in response to the stimulus with the largest amplitude (3.6 mm) in the various lamina (indicated to the left of the panel). Recordings are from sham surgery animals and from locations contralateral (contra) and ipsilateral (ipsi) to the LFPI site. Each Grand peristimulus time histogram was generated by averaging responses across all responsive clusters within that lamina. The grey-shaded box represents the analysis window used to extract response metrics. (**B**) Peak firing rate extracted from the onset response to the stimuli, from clusters ipsilateral to the site of injury (white circles), contralateral to the site of injury (grey circles), and in sham animals (black circles). Data represent averages from all responsive clusters (± standard error of the mean) at all tested ramp velocities, separated by cortical lamina (* = ipsilateral vs. sham; $p < 0.05$).

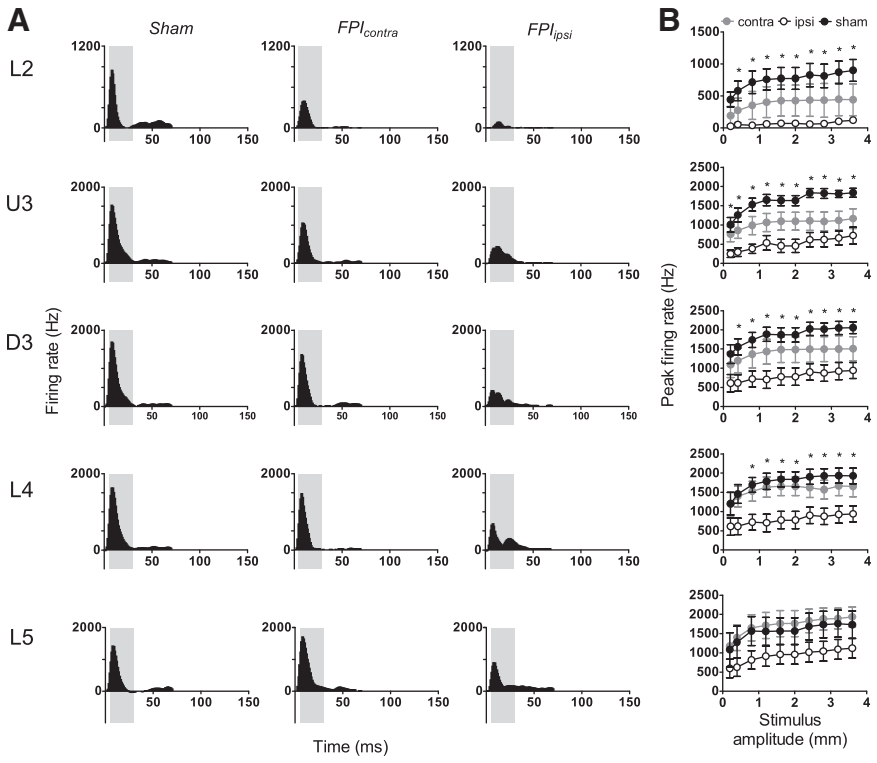

FIG. 3. Mild lateral fluid percussion injury (LFPI) effects on pattern and strength of multiunit cluster responses evoked by complex rough surface discrimination stimuli. Population peristimulus time histograms are shown in (**A**) in response to the stimulus with the largest amplitude (3.6 mm) in the various lamina (indicated to the left of the panel). Recordings are from sham surgery animals, and from locations contralateral (contra) and ipsilateral (ipsi) to the LFPI site. Each Grand peristimulus time histogram was generated by averaging responses across all responsive clusters within that lamina. The grey-shaded box represents the analysis window used to extract response metrics. (**B**) Peak firing rate extracted from the onset response to the stimuli, from clusters ipsilateral to the site of injury (white circles), contralateral to the site of injury (grey circles), and in sham animals (black circles). Data represent averages from all responsive clusters (±standard error of the mean) at all tested ramp velocities, separated by cortical lamina (*=ipsilateral vs. sham; $p<0.05$).

visual impressions gained from the Grand PSTHs in Figure 3A. In barrel cortex ipsilateral to the mild LFPI, there was found a significant suppression of the population peak firing rate in all layers except Layer 5 (two-way ANOVA, $p<0.05$) when compared with population peak firing rate in sham surgery controls. There was no significant difference between peak firing rates at any velocity in any layer in the contralateral barrel cortex compared with sham controls.

Single cell responses to whisker motion after mild LFPI

To assess responses from individual cells, single cell responses were spike-sorted from multineuron clusters as described in Methods. We analyzed two metrics from all responsive single cells for both simple and complex whisker stimuli: (1) peak excitatory firing rate and (2) latency to the peak excitatory firing rate, using the same analysis windows as applied to the population responses as detailed above (5–50 msec for the trapezoid and object contact stimuli; 5–30 msec for the rough surface discrimination waveform stimuli).

Responsiveness to trapezoidal motion

Responses evoked by the simple trapezoidal stimulus were obtained (Fig. 4A) from 99 responsive single cells in barrel cortex ipsilateral to the mild LFPI, 123 responsive single cells in barrel cortex contralateral to the mild LFPI, and 254 responsive single cells in barrel cortex of sham surgery controls. Mild LFPI-induced response suppression was as pervasive in the single cells as in the population response, and a significant reduction in peak firing rate at all stimulus velocities was found in Layers 2, 4, and 5 in barrel cortex ipsilateral to the injury site compared with the same layers in sham surgery controls (Fig. 4A; two-way ANOVA, $p<0.05$); no change in single cell firing rate was found in Upper Layer 3 or Deep Layer 3 of the barrel cortex.

Comparing the single cell responses in the barrel cortex contralateral to the mild LFPI with sham surgery control responses, there was a significant increase in peak firing rate at most trapezoidal ramp velocities in Upper Layer 3 (Fig. 4A; two-way ANOVA, $p<0.05$). No other systematic differences in firing rate were found in the barrel cortex contralateral to the injury site compared with the sham surgery controls.

With respect to the timing of responses, as indexed by the latency to the peak firing rate, in cells in barrel cortex ipsilateral to the mild LFPI, there was a significant increase in latency to peak firing rate in Layer 4 compared with sham surgery controls (Fig. 5A; two-way ANOVA, $p<0.05$), but not in any other layers. With respect to the timing of responses in the contralateral barrel cortex versus that in sham surgery controls, there were significant differences in the latency to peak firing rate only in Layer 2 and Layer 5 (Fig. 5A; two-way ANOVA, $p<0.05$).

Responsiveness to object contact motion

Responses evoked by the complex object contact whisker motion were obtained from 123 responsive cells in the barrel cortex

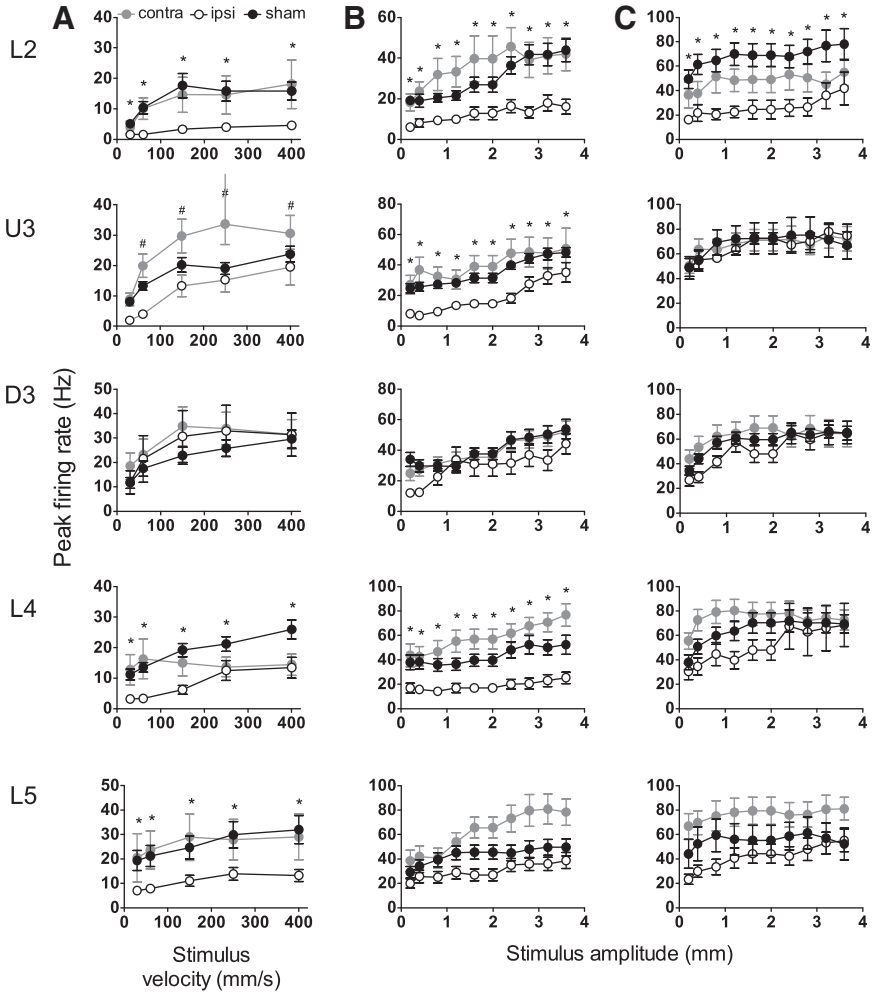

FIG. 4. Mild lateral fluid percussion injury (LFPI) effects on strength of single cell responses evoked by simple and complex whisker stimuli. Single cell metrics were extracted from the same analysis windows as for Figures 1–3. Peak firing rate changes in response to the trapezoidal stimuli (**A**), object contact stimuli (**B**), and rough surface discrimination stimuli (**C**) in the various cortical lamina (indicated to the left of the panel). Recordings are from cells ipsilateral (ipsi) to the site of injury (white circles), contralateral (contra) to the site of injury (grey circles), and in sham animals (black circles). Data represent averages from all responsive cells (±standard error of the mean) at all tested stimulus velocities and amplitudes (* = ipsilateral vs. sham; # = contralateral vs. sham; $p < 0.05$).

ipsilateral to the mild LFPI site, 134 responsive single cells in the barrel cortex contralateral to the mild LFPI site, and 222 responsive single cells in the barrel cortex in sham surgery controls. In barrel cortex ipsilateral to the mild LFPI, there was a significant reduction in peak firing rate in all layers except Deep Layer 3 and Layer 5 (Fig. 4B; two-way ANOVA, $p < 0.05$). Single cell response rates in barrel cortex contralateral to the mild LFPI were not different from those in the equivalent layers in sham surgery controls. Finally, significant changes in the latency to peak firing rate were only recorded in Deep Layer 3, where an increased latency was recorded in cells ipsilateral to the site of mild LFPI relative to latencies in sham surgery controls (Fig. 5B; two-way ANOVA, $p < 0.05$).

Responsiveness to rough surface discrimination motion. Responses evoked by the complex rough surface discrimination motion were obtained from 123 responsive cells in the barrel cortex ipsilateral to the mild LFPI site, 123 responsive single cells in the barrel cortex contralateral to the mild LFPI site, and 115 responsive single cells in the barrel cortex in sham surgery animals. A reduction in peak firing rate in cells in barrel cortex ipsilateral to the mild LFPI compared with sham surgery controls was found in Layer 2 only (Fig. 4C; two-way ANOVA, $p < 0.05$). In all other layers, ipsilateral response rates remained unchanged by mild LFPI. Comparing responses in barrel cortex contralateral to the mild LFPI and those in barrel cortex in sham surgery animals, again there were no significant differences in peak firing rate in any cortical layer (Fig. 4C). A significant increase in the latency to peak firing rate was found in all layers except Layer 2 in barrel cortex ipsilateral to the mild LFPI compared with barrel cortex in sham surgery controls (Fig. 5C; two-way ANOVA, $p < 0.05$); there was generally no significant difference in latency to peak firing rate in barrel cortex contralateral to the mild LFPI compared with barrel cortex in sham surgery controls (Fig. 5C), except for a decrease in the latency in Layer 4 (two-way ANOVA, $p < 0.05$).

We have previously demonstrated an enhanced spontaneous output in Layer 4 and Layer 5 of cortex in the acute period after mild TBI induced with the WDIA method.[18] To assess whether the mild LFPI method of injury induced similar changes, spontaneous firing rate (recorded in the 200 msec window before stimulus onset) was extracted from the single cell data for both ipsilateral and contralateral recordings in mild LFPI animals, and in sham animals. As in our

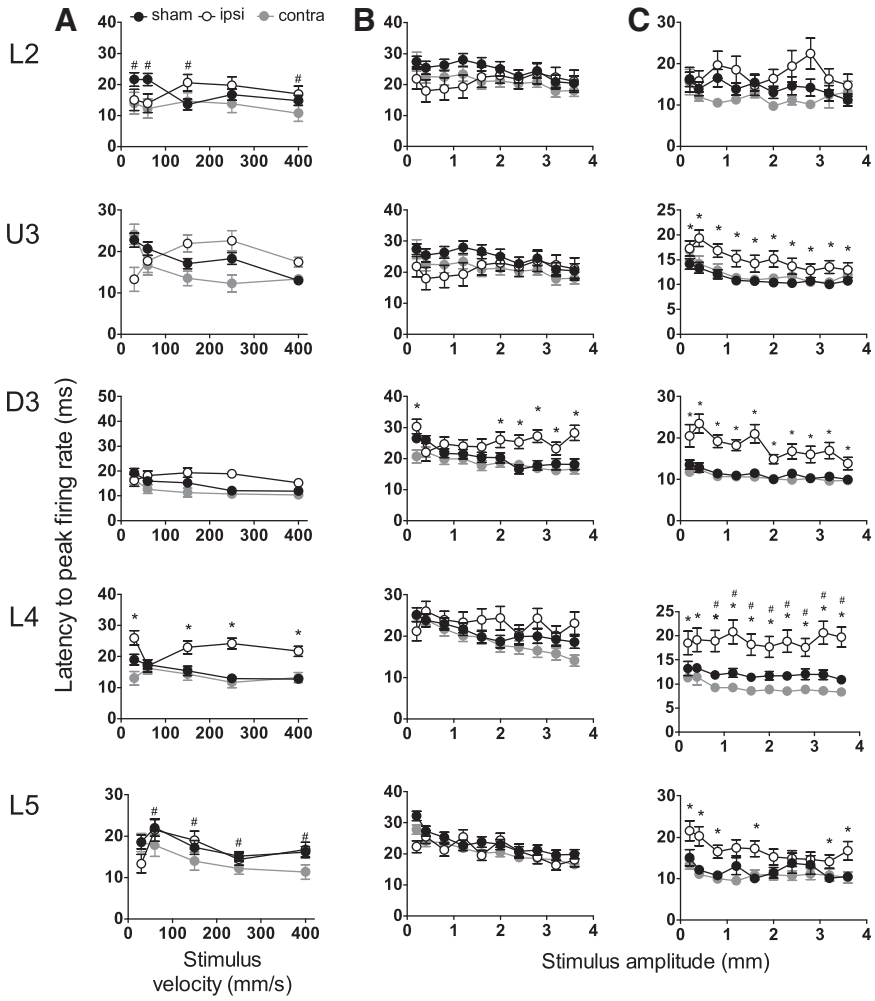

FIG. 5. Mild lateral fluid percussion injury (LFPI) effects on timing of single cell responses evoked by simple and complex whisker stimuli. Single cell metrics were extracted from the same analysis windows as for Figures 1–3. Latency to peak firing rate in response to the trapezoidal stimuli (**A**), object contact stimuli (**B**), and rough surface discrimination stimuli (**C**) is shown in the various cortical lamina (indicated to the left of the panel). Recordings are from cells ipsilateral (ipsi) to the site of injury (white circles), contralateral (contra) to the site of injury (grey circles), and in sham animals (black circles). Data represent averages from all responsive cells (± standrd error of the mean) at all tested stimulus velocities and amplitudes (* = ipsilateral vs. sham; # = contralateral vs. sham; $p < 0.05$).

previous study using the WDIA injury method to create diffuse TBI, an elevation in spontaneous output was measured in Layer 5a only, and only in recordings ipsilateral to the mild LFPI site (Fig. 6; ipsi = 0.397 ± 0.06 Hz; contra = 0.02 ± 0.003 Hz; sham = 0.09 ± 0.009 Hz; two-way ANOVA, $p < 0.05$), with spontaneous firing rate returning to normal levels in Layer 5b. No change in spontaneous output was measured in the hemisphere contralateral to the mild LFPI, or in sham surgery control animals.

Summary of electrophysiological recordings

In general, there was a suppression of multiunit responses to all stimuli in Layer 2 through to Layer 5 with ipsilateral mild LFPI recordings compared with recordings in sham surgery animals and a similar suppression of single-cell responses to all stimuli in most cortical layers with ipsilateral mild LFPI recordings, except for Deep Layer 3, which showed an absence of change in response to all stimuli (Fig. 7). This was true regardless of stimulus type; the hypoexcitable state of the network persisted in the face of various types of afferent information, each of which evoked a unique and reproducible pattern of neuronal output from the barrel network. This suggests that complexity of afferent information does not affect perturbations in signal processing and integration during the acute phase after a mixed focal/diffuse model of injury. While there was a general trend toward a suppression of neuronal responsiveness contralateral to the site of mild LFPI, this was not significant at either the single unit or population level. In addition, an elevation in spontaneous output was noted in Layer 5a only, and only at sites ipsilateral to the injury locus.

Immunohistochemistry

Extensive NF-200 positive axons and dendrites were observed in the cingulum and external capsule in the hemisphere ipsilateral to the mild LFPI. Positive NF-200 appeared in the cell body, short and long processes, and accumulated into bulbs (Fig. 8B,C) indicating axonal transporting impairment at 24 h after mild LFPI. NF-200 positive cell bodies and axons were also observed in the grey and white matter of somatosensory cortex (Fig. 8D,E). In comparison, no NF-200 positive staining was observed in the hemisphere contralateral to the mild

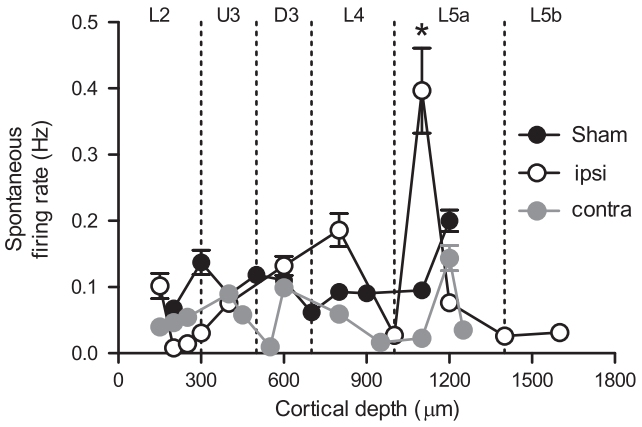

FIG. 6. Enhanced spontaneous output in Layer 5a ipsilateral to the lateral fluid percussion injury (LFPI) site. Spontaneous firing rate was measured in the 200 msec window before stimulus onset and was extracted from single unit data for mild LFPI and sham animals. Mean (±standard error of the mean) spontaneous firing rate is shown according to depth from cortical surface, with depth demarcated into cortical lamina. Enhanced spontaneous output was observed in recordings ipsilateral (ipsi) to the mild LFPI site in Layer 5a of the cortex, with no change in the contralateral (contra) hemisphere (*$p < 0.05$).

LFPI, or in sham animals (Fig. 8F,G). Quantification of the number of NF-positive cells (Fig. 8H) showed significant differences between the mild LFPI and sham animals for the two broad sets of areas (Mann Whitney U test, $p < 0.05$) but only in the hemisphere ipsilateral to the injury site and not contralaterally.

Discussion

The development of effective treatments for patients with TBI necessitates an understanding of how the interplay between primary and secondary injury mechanisms in the acute stages of injury progress into long-term functional changes. It is therefore of paramount importance that TBI be studied in an experimental setting to gain further insight into the injury-induced changes in neuronal function that underlie behavioral and cognitive deficits. Rodent models of TBI are the current benchmark for study in the laboratory setting, with a primary aim to reproduce clinically relevant patterns of brain injury observed in humans.[3,9]

This is the first study to detail electrophysiological changes in rodent sensory cortex after a combined diffuse and focal brain injury, induced using the LFPI model. At both the population and single cell level, the effects on neuronal responses after this form of injury are remarkably similar to those we have previously described after diffuse-only injury.[18,19] One important point of note is that we found a global hypoactivity that was independent of stimulus type—and that was similar to what we have found previously in the acute phase of a different TBI model.[18] This demonstrates that signaling cascades that dominate during the acute phase of injury are common between different injury models and must then diverge at a later time point to account for different functional outcomes.

Distance dependency of post-injury neuronal responses is similar between different injury models involving impact to the brain

In this study, LFPI was used to induce mild TBI using similar FPI parameters as have previously been used.[9,28,30,38] Similar to these studies, we also report that mild FPI produced no apnea or loss of consciousness, but did induce a delay in recovery time of the self-righting reflex. Then, 24 h after the mild LFPI, when behaviors appeared to be normal, there was still an overall suppression of sensory cortical neuronal responses, but only in the ipsilateral hemisphere. Although firing rates in the contralateral hemisphere were intermediate between ipsilateral and sham responses, they were not significantly different from peak firing rates in sham animals.

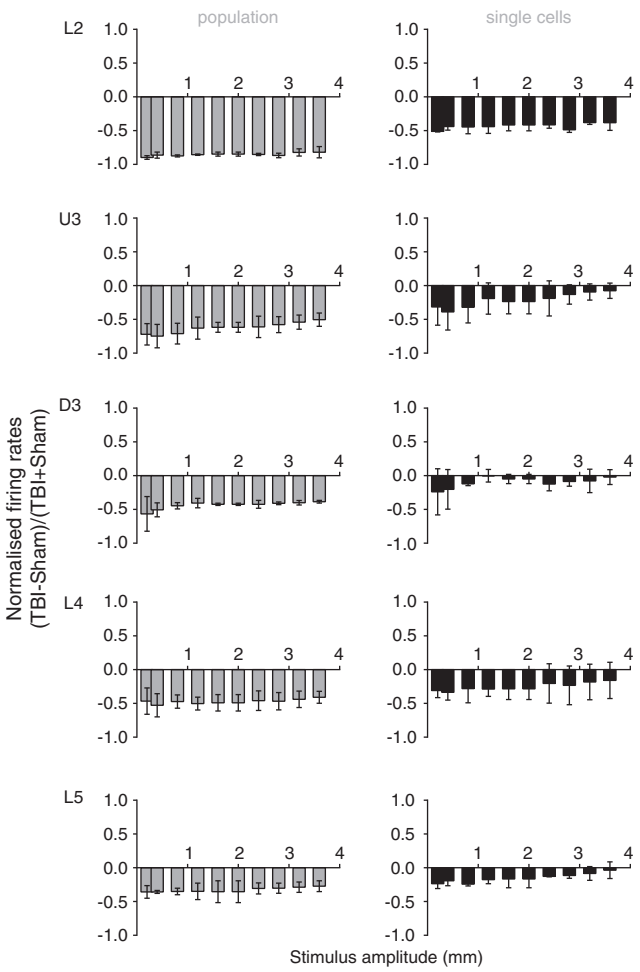

FIG. 7. Summary of effects of mild lateral fluid percussion injury (LFPI) in the ipsilateral barrel cortex at the population level (left column) and at the single cell level (right column) for the two complex naturalistic stimuli. At each amplitude of each of the two naturalistic stimuli (see text), we calculated for each cortical lamina the normalized peak firing rate in the mild LFPI for ipsilateral recordings with resepect to those made in sham animals. The two normalized values (one for each stimulus) were used to calculate the mean normalized peak firing rate and SD, which are presented here for each cortical lamina (L2 = layer 2; U3 = Upper Layer 3; D3 = Deep Layer 3; L4 = Layer 4; L5 = Layer 5). A value of zero indicated equal firing rates (ratio of 1) in the two groups, with negative values indicating a neuronal suppression and positive values indicating an enhancement of activity. In the population data, there was strong suppression of firing rates in mild LFPI animals (ratios < 0) with a depth dependency to the suppression, being greatest most superficially in cortex (L2) and least deep in cortex (L5). Similar trends were seen in the single unit data, although the suppression in the cells from which recordings were obtained was less than in the population in the same lamina.

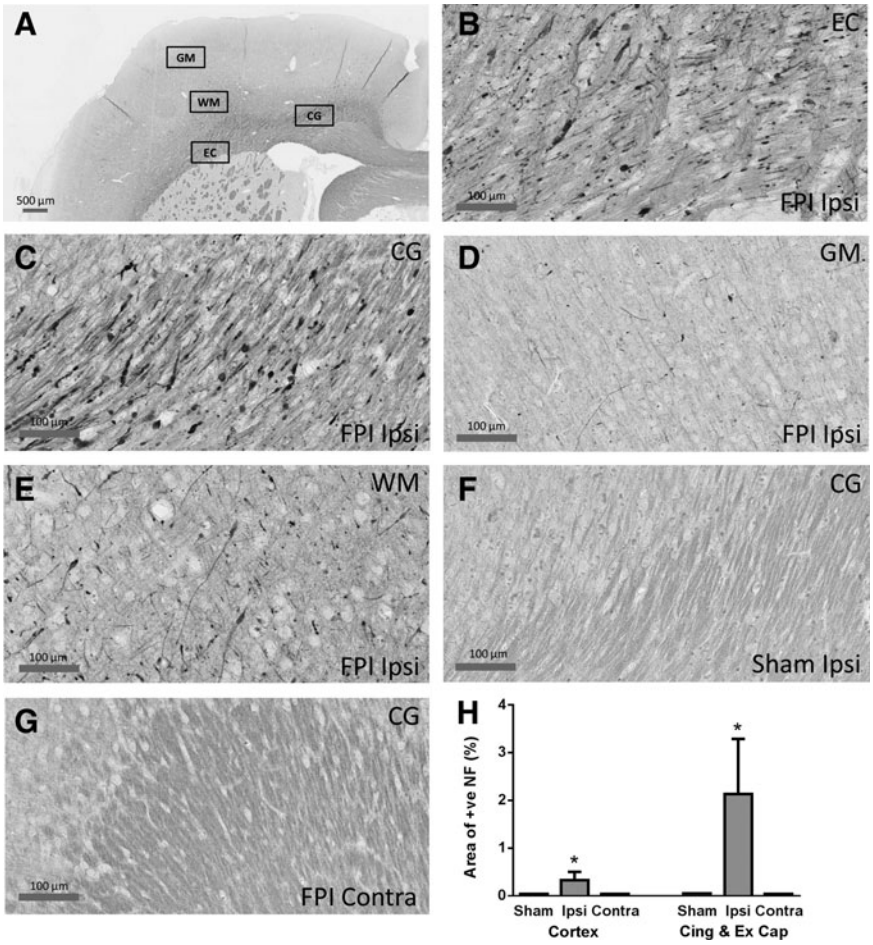

FIG. 8. NF-200 staining in the hemisphere ipsilateral to the mild lateral fluid percussion injury (LFPI). (**A**) shows the four regions of the brain examined for NF-200 staining for axonal injury; GM = grey matter (of cortex), WM = white matter (of cortex), EC = external capsule, CG = cingulum. (**B–E**): In the cortex ipsilateral to the mild LFPI, NF positive axons and dendrites were observed in the external capsule (B), cingulum (C), and white matter below the barrel cortex (E), but were barely discernible in the grey matter of the barrel cortex (D). No staining was found in the sham surgery animals (**F**: cingulum) or in the cortex contralateral to the mild LFPI (**G**: cinglulum). NF-200 staining was detected in the cell body, short and long processes and accumulated into bulbs (B,C). (**H**) Quantification of NF positivity. Densitometric analysis was used to calculate the total area stained for NF-200 within a region of interest (ROI), and this was expressed as a percentage of the total area within the ROI. Asterisks indicate that significant differences were found between sham animals and the mild LFPI animals for structures in the ipsilateral (ipsi) hemisphere but not for structures in the contralateral (contra) hemisphere.

In agreement with these electrophysiological observations, histological analysis found that neuronal and axonal injuries also occurred only ipsilateral to the mild LFPI, as also reported in previous histological and anatomical studies of mild LFPI,[22,28,39] in comparison with mild LFPI delivered at midline and parasaggital locations that cause bilateral cortical changes.[12] The only previous report of electrophysiological recordings in mild LFPI also reported a reduction in the size of the vibrissae-stimulation induced population response in barrel cortex at 72 h post-injury, but no differentiation between different cortical lamina was attempted in that study for the electrophysiology.[38]

Our observation of a depth-dependent decrease in depression of cortical responses (as in the case of the WDIA diffuse model of injury model in which impact force is distributed across the entire cortical surface) in the ipsilateral hemisphere provides an explanation for the absence of significant effects on contralateral neuronal responses. These results suggest that suppression of neuronal activities is likely to be dependent on distance from the impact site, with contralateral sites far from the injury point exhibiting only a small hypoactivity (as demonstrated by a trend toward significance, evidenced by a p value close to 0.05 in many comparisons).

This is consistent with the hypothesis that a stress/strain wave emanates from the point of injury[40–43] and (as proposed in our previous study using a diffuse-only injury model[18]) causes a suppression of activity within the immediate post-injury period that dissipates with distance from the impact site. This would account for our previous observations of a lamina-specific pattern of suppression, with more superficial cortical layers demonstrating a greater degree of suppression than deeper layers.[18,19] A similar rationale may apply to the LFPI model with the stress wave generated by the fluid impulse inducing a distance-dependent suppression from the lateral point of impact, and this is sufficiently weaker by the contralateral side to produce nonsignificant changes in that hemisphere.

These observations are consistent with the pattern of stresses and deformations seen in rat brain models subject to head impact

injury.[40,41,43] In these models, impact injury applied via a craniectomy or to the outside of the closed head creates stresses/strains that propagate from the surface toward deeper structures in the diencephalon and mesencephalon.[40,41] Models that acknowledge the complex properties of different brain structures, transitions between structures (e.g., between grey and white matter), and the different types of stress, pressure, compression, and elastic waves[44] show that such dependencies are not related only to distance: thus, in the model of Lamy and associates,[41] of the three test brain areas, the hypothalamus (the most distant area) suffered slightly higher strains and stresses than the parietal cortex (the most proximate area), but values in thalamus were substantially lower.

Nevertheless, as a working generalization, stresses and strains can be treated as decreasing with distance from the impact site,[40,43] and the models consistently indicate that with unilateral injury (as in the LFPI method used here), brain deformations or strains from head impact are substantially lower in the contralateral than in the ipsilateral hemisphere.[40,43] Similar effects are seen in models of human impact brain injury,[11,45] albeit with some modifications for the fact that the absence of sulci in the rat brain may alter the exact mechanics of brain impact injury.[46]

One feature of the present results not predicted by the rat brain injury models is that neuronal responses in the contralateral hemisphere, although not significantly different from normal responses, also trended toward a decrease in neuronal response in all cortical layers. This does not accord with the pattern of propagation of the stress/strain waves predicted in the rat brain injury models.[40,41,43] As noted above, in these models the propagation of stress/strain waves from a unilateral injury occurs from that site into the depth of the brain in a manner that dissipates with distance, not a surface wave as would be needed to produce a contralateral injury that decreases from supragranular to infragranular laminae on that side of the head. An exception is seen when unilateral impact injury is coupled with bilateral craniotomies,[43] which produces a dominant injury focus at the cortical site of impact and a second weaker one in the cortex in the other hemisphere,[43] with both areas showing a (non-linear) depth-dependent decrease in effects from the cortical surface.

Only a unilateral craniotomy, however, was made in our case, so this could not account for the fact that our present data also suggest two foci of injuries (one in each hemisphere) with a depth dependent decrease from surface to deep layers in the effects on cortical neurons. We propose that this likely reflects that a unilateral mild LFPI causes brain displacement to hit the cranium (''contre-coup'' effect) on the opposite side to the impact itself. This blow to the contralateral hemisphere appears to result in similar consequences, albeit in a much attenuated fashion, of a depth-dependent decrease in neuronal response changes from contralateral cortical surface to depth.

Similarities and differences in effects at single cell compared with population level

Effects at the single cell level were very similar to those seen in population responses with a general suppression of single cell activity, and this effect was predominantly observed in the recording site ipsilateral to the injury, with little to no change in contralateral responses. With regard to changes in response timing, although the results were somewhat inconsistent, there was a general pattern of longer latencies, particularly in Deep Layer 3 and Layer 4. These changes were more pronounced in responses evoked by complex stimuli, where latency shifts of up to 10 msec were apparent in some instances.

Similar increases in response latency have been previously reported by Sanders and colleagues,[38] who demonstrated that longer latencies recorded in the barrel cortex field potentials after a similar mild FPI were coupled with impaired exploratory activity in an open-field water maze task, presumably as a result of dysfunctional circuitry and neuronal output within the whisker cortex. Although in their study no attempt was made to discriminate between cortical lamina, and in our study we did not directly measure vibrissal function, it is reasonable to speculate that comparable impairments might exist in these animals, given the similar shift in response timing reported in both studies.

Overall, effects on firing activity at the single unit level were never as severe as the effects at the population level, even in Layer 2 where effects at both levels were substantial. This suggests that the injury impacts differentially in the short term on different cells—i.e., that specific subtypes of cortical cells exhibit different vulnerability to injury. Then, the cells we are likely to record from in extracellular recordings (larger pyramidal neurons are likely to be the dominant cell type for such recordings[31,32]) may be less affected than other cells (excitatory cells such as spiny stellate cells and inhibitory interneurons).

In support of this hypothesis, we found a substantive difference between population and single cells in Deep Layer 3: suppression of responses was absent in single cells in Deep Layer 3, but not in the population responses from this layer. Deep Layer 3 in the barrel cortex contains a high density of interneurons (which are primarily parvalbumin- and somatostatin-positive[47]) and in culture preparations, these interneuronal subtypes are preferentially damaged after excitotoxic insult, as occurs in the aftermath of brain injury.[48] It is true that Layer 2 and Layer 5a also contain dense populations of interneurons,[47] yet we found significant single cell and population hypoactivity here.

Susceptibility to injury is likely dictated by a combination of cell characteristics (that determine vulnerability) and proximity to the insult.[11] By this argument, pyramidal cells and interneurons in Layer 2 and possibly Upper Layer 3 may be equally rendered nonfunctional, whereas both cell classes in Layer 5 may largely be spared from damage. In contrast, in Deep Layer 3 the injury-susceptible interneurons alone may be damaged while pyramidal neurons are largely spared. Given the feed-forward projections from Layers 2 and Upper Layer 3 to Layer 5,[49] these events would result in hypoactivity in both Layers 2 and 5, with no change in Deep Layer 3 as we report here. This remains a testable hypothesis, and we have commenced studies on identifying through immunohistochemistry if this hypothesis can be substantiated.

Finally, we previously reported an increase in spontaneous discharge in single cells within Layer 5a of barrel cortex 24 h after severe diffuse injury, but without any associated changes in net excitability.[18] In the present study, too, we found an increase in spontaneous discharge within Layer 5a of the ipsilateral cortex, again with no significant changes in net excitability. Changes in spontaneous output have previously been recorded in the acute period after TBI[50–52] and are frequently associated with large scale changes in network connectivity after injury.[53,54]

Although the majority of inputs to Layer 5a arise from Layers 2 and 3 of cortex, there are two alternate afferent inputs to Layer 5a that may also provide the enhanced spontaneous drive we report here. Small thalamic inputs from the medial posterior nucleus (POm) are known to innervate Layer 5a via the paralemniscal sensory pathway,[55] and Layer 4 spiny stellate cells also provide selective input to Layer 5a.[56,57] While we can only speculate about the origin of this enhanced spontaneous output, it is nonetheless

clear that this change in drive is likely to be a precursor in establishing the dynamic changes in circuitry that are known to occur in the early stages post-TBI.[58]

It is worth noting that the extent of increase in spontaneous output was lower after mild FPI here than we previously reported after severe diffuse-only injury (spontaneous activity changes were not monitored in our study of immediate post-injury effects after mild diffuse TBI[19]). This presumably reflects the differing severity between the two studies, but nevertheless reinforces the similarity in immediate post-injury processes in both models, despite the differences in method of injury and long-term outcomes (discussed below).

Neuronal mechanisms underlying immediate post-injury neuronal suppression

It is difficult to elucidate the exact cellular mechanisms that underlie the depression we observed in both injury models; however, given the common factor of distance-dependent response depression, a first step in the pathway may be a wave of cortical spreading depression (CSD). CSD is a well-documented phenomenon characterized by a rapid and almost complete depolarization of large populations of neurons, with global redistribution of ions between intracellular and extracellular compartments that propagates as a wave in brain tissue in a regenerative fashion.[59] The wave spreads at a uniform speed of a few millimetres per minute[60–62] with the leading edge of the wave in layers containing apical dendrites.[63] If the depolarization persists for long enough, neurons enter an ''unresponsive'' state and can be rendered hypoactive in the long term.[62]

The processes that allow for persistence of this depression beyond a few hours are unknown; however, given the known link between CSD and cortical plasticity,[64] it seems likely that synaptic events such as long-term depression may be important. Cortical waves of depression have been monitored after injury induced with predominantly focal injury models, such as the LFPI,[65–68] Feeney's weight drop,[69] and the controlled cortical impact (CCI) model,[70] but have yet to be documented after a diffuse model of injury, such as the WDIA model. Nevertheless, our findings suggest that CSD is likely to be an important phenomenon after both diffuse and focal forms of injury, and may be important in establishing persistent cortical cellular changes. Such a hypothesis would also likely explain the independence of these effects on stimulus complexity, because the nature of incoming information is unlikely to impact neuronal output in a circuit that has been overwhelmed by a dominating quiescence.

Similar post-injury cortical effects diverge to produce different long-term behavior consequences

The similarities between the findings of this study and our previous study on mild diffuse-only injury[19] suggest that there must be shared injury mechanisms in the immediate post-injury period that are important in establishing the behavioral deficits associated with each injury model. The two injury models, however, induce very different long-term histopathologies and can produce different long-term behavioral outcomes.[9,22,71,72] The LFPI model frequently induces post-traumatic seizures,[23,24,73] which has been attributed to persistent hyperexcitability within the cortex.[74] We have demonstrated long-term cortical hyperexcitability after WDIA-induced injury,[17] but this occurs in the absence of seizure activity in this diffuse injury model. One point to note here is that we applied only mild FPI in this study, and that development of post-traumatic epilepsy is often thought to be dependent on injury severity.[75] An additional phenotypic difference between the two models is that injury induced using the LFPI model results in more persistent sensorimotor deficits with a larger extent of neuronal degeneration within the cortex than is seen after WDIA-induced injury.[22]

It would be simple to assume then that the similar short-term neuronal consequences in both models[18,19] reflect the primary mechanical-injury dependent consequences of the impact, and we predict that there may then be a subsequent divergence in long-term neuronal consequences that reflects a divergence of the injury cascades in secondary injury processes. We examined the neuronal effects 24 h after injury; while it is true that some secondary injury processes only begin after this period,[7] other secondary injury processes begin within hours of injury.[7,11,76]

A series of elegant studies by Povlishock and colleagues[77–80] has shown that traumatic axonal injury consists of a continuous series of changes in axonal pathology from 5 min post-trauma through to 30 days post-trauma. Our data on the similarity of neuronal outcomes with the two models, however, indicates that the processes affecting neuronal responses in the first 24 h are likely to be common to both models, and it seems most parsimonious to assume that they are all derived directly from the primary injury processes.

Implications of the results

It is generally acknowledged that mild TBI is difficult to diagnose, even in the immediate post-injury period because deficits, even at the behavioral and structural (imaging) level, are difficult to identify.[11] Our results are certainly concordant with that observation. because only mild deficits, in the self-righting reflex, were seen immediately after the mild LFPI used here, as in previous studies of mild LFPI.[27,28,38] It is then very encouraging to note, however, that mild changes in neuronal responsiveness and latency at the single cell level translated to significant substantial changes in neuronal responsiveness of the population, especially on the ipsilateral side; on the contralateral side, even though population effects were not significant, there was a trend that followed the same pattern as on the ipsilateral side.

The amplification of single cell effects to the responses at the population level is very encouraging in suggesting that cortical evoked potentials might be useful in evaluating mild TBI, as proposed previously.[11] Such techniques may provide a more sensitive means of diagnosing mild TBI and monitoring recovery, and could be particularly useful in the sports and military setting where repeated mild concussive blows are common, may result in long-term neurological consequences,[81,82] and are known to induce cumulative behavioural and neuropathological changes.[27]

Although we have only monitored the effects of mild TBI in the acute phase after injury here (and in our previous study[19]), it is likely that the imbalances in neuronal activity that we report would recover in the long term. Any subsequent mild concussive events occurring during this recovery period, however, would likely predispose already vulnerable networks to more severe dysfunction.[83,84] Our future studies will explore the recording of evoked potentials in this setting to determine if, despite reservations in the literature,[85] carefully selected electrical measures of cortical activity could index single and repetitive mild TBI events and recovery.

Finally, it is worth emphasizing the fact that similar short-term cortical neuronal depression in the two models we have studied

electrophysiologically, one causing only diffuse injury [19] and the present one causing a mixture of diffuse and focal injury, diverges to different histopathologies and behavior outcomes. This highlights the importance of considering targeting drugs appropriately not only to the selected therapeutic window, but also as a function of injury type.

Acknowledgments

This work was supported by the National Health and Medical Research Council of Australia (grant numbers APP1029311, APP1006077) and a research fellowship from the Canadian Institutes of Health Research.

Author Disclosure Statement

No competing financial interests exist.

References

1. Murray, C.J., and Lopez, A.D. (1996). *Global Health Statistics: A Compendium Of Incidence, Prevalence, And Mortality Estimates For Over 200 Conditions*. Harvard University Press: Cambridge, MA.
2. Povlishock, J.T., and Katz, D.I. (2005). Update of neuropathology and neurological recovery after traumatic brain injury. J. Head Trauma Rehabil. 20, 76–94.
3. Morganti-Kossmann, M.C., Yan, E., and Bye, N. (2010). Animal models of traumatic brain injury: is there an optimal model to reproduce human brain injury in the laboratory? Injury 41, Suppl 1, S10–S13.
4. Gennarelli, T.A., Thibault, L.E., Adams, J.H., Graham, D.I., Thompson, C.J., and Marcincin, R.P. (1982). Diffuse axonal injury and traumatic coma in the primate. Ann. Neurol. 12, 564–574.
5. Gennarelli, T.A. (1983). Head injury in man and experimental animals: clinical aspects. Acta Neurochir. Suppl. (Wein) 32, 1–13.
6. Graham, D.I., McIntosh, T.K., Maxwell, W.L., and Nicoll, J.A. (2000). Recent advances in neurotrauma. J. Neuropathol. Exp. Neurol. 59, 641–651.
7. Werner, C., and Engelhard, K. (2007). Pathophysiology of traumatic brain injury. Br. J. Anaesth. 99, 4–9.
8. Alwis, D.S., Johnstone, V., Yan, E., and Rajan, R. (2013). Diffuse traumatic brain injury and the sensory brain. Clin. Exp. Pharmacol. Physiol. 40, 473–483.
9. Xiong, Y., Mahmood, A., and Chopp, M. (2013). Animal models of traumatic brain injury. Nat. Rev. Neurosci. 14, 128–142.
10. Greve, M.W., and Zink, B.J. (2009). Pathophysiology of traumatic brain injury. Mt. Sinai J. Med. 76, 97–104.
11. Gaetz, M. (2004). The neurophysiology of brain injury. Clin. Neurophysiol. 115, 4–18.
12. Cernak, I. (2005). Animal models of head trauma. NeuroRx. 2, 410–422.
13. Davis, A.E. (2000). Mechanisms of traumatic brain injury: biomechanical, structural and cellular considerations. Crit. Care Nurs. Q. 23, 1–13.
14. McIntosh, T.K., Smith, D.H., Meaney, D.F., Kotapka, M.J., Gennarelli, T.A., and Graham, D.I. (1996). Neuropathological sequelae of traumatic brain injury: relationship to neurochemical and biomechanical mechanisms. Lab. Invest. 74, 315–342.
15. Rosenfeld, J.V., Maas, A.I., Bragge, P., Morganti-Kossmann, M.C., Manley, G.T., and Gruen, R.L. (2012). Early management of severe traumatic brain injury. Lancet 380, 1088–1098.
16. Ding, M.C., Wang, Q., Lo, E.H., and Stanley, G.B. (2011). Cortical excitation and inhibition following focal traumatic brain injury. J. Neurosci. 31, 14085–14094.
17. Alwis, D., Yan, E.B., Morganti-Kossmann, M.C., and Rajan, R. (2012). Sensory cortex underpinnings of traumatic brain injury deficits. PLoS One 7, e52169.
18. Johnstone, V.P., Yan, E.B., Alwis, D.S., and Rajan, R. (2013). Cortical hypoexcitation defines neuronal responses in the immediate aftermath of traumatic brain injury. PloS One 8, e63454.
19. Yan, E.B., Johnstone, V.P., Alwis, D.S., Morganti-Kossmann, M.C., and Rajan, R. (2013). Characterising effects of impact velocity on brain and behaviour in a model of diffuse traumatic axonal injury. Neuroscience 248C, 17–29.
20. Marmarou, A., Foda, M.A., van den Brink, W., Campbell, J., Kita, H., and Demtriadou K. (1994). A new model of diffuse brain injury in rats. Part I: Pathophysiology and biomechanics. J. Neurosurg. 80, 291–300.
21. Gilchrist, M.D. (2004). Experimental device for simulating traumatic brain injury resulting from linear accelerations. Strain 40, 180–192.
22. Hallam, T.M., Floyd, C.L., Folkerts, M.M., Lee, L.L., Gong, Q.Z., Lyeth, B.G., Muizelaar, J.P., and Berman, R.F. (2004). Comparison of behavioral deficits and acute neuronal degeneration in rat lateral fluid percussion and weight-drop brain injury models. J. Neurotrauma 21, 521–539.
23. Mukherjee, S., Zeitouni, S., Cavarsan, C.F., and Shapiro, L.A. (2013). Increased seizure susceptibility in mice 30 days after fluid percussion injury. Front. Neurol. 4, 28.
24. Shultz, S.R., Cardamone, L., Liu, Y.R., Hogan, R.E., Maccotta, L., Wright, D.K., Zheng, P., Koe, A., Gregoire, M.C., Williams, J.P., Hicks, R.J., Jones, N.C., Myers, D.E., O'Brien, T.J., and Bouilleret, V. (2013). Can structural or functional changes following traumatic brain injury in the rat predict epileptic outcome? Epilepsia 54, 1240–1250.
25. Jones, N.C., Cardamone, L., Williams, J.P., Salzberg, M.R., Myers, D., and O'Brien, T.J. (2008). Experimental traumatic brain injury induces a pervasive hyperanxious phenotype in rats. J. Neurotrauma 25, 1367–1374.
26. Liu, Y.R., Cardamone, L., Hogan, R.E., Gregoire, M.C., Williams, J.P., Hicks, R.J., Binns, D., Koe, A., Jones, N.C., Myers, D.E., O'Brien, T.J., and Bouilleret, V. (2010). Progressive metabolic and structural cerebral perturbations after traumatic brain injury: an in vivo imaging study in the rat. J. Nucl. Med. 51, 1788–1795.
27. Shultz, S.R., Bao, F., Omana, V., Chiu, C., Brown, A., and Cain, D.P. (2012). Repeated mild lateral fluid percussion brain injury in the rat causes cumulative long-term behavioral impairments, neuroinflammation, and cortical loss in an animal model of repeated concussion. J. Neurotrauma 29, 281–294.
28. Shultz, S.R., MacFabe, D.F., Foley, K.A., Taylor, R., and Cain, D.P. (2011). A single mild fluid percussion injury induces short-term behavioral and neuropathological changes in the Long-Evans rat: support for an animal model of concussion. Behav. Brain Res. 224, 326–335.
29. Shultz, S. R., Bao, F., Weaver, L. C., Cain, D. P., and Brown, A. (2013). Treatment with an anti-CD11d integrin antibody reduces neuroinflammation and improves outcome in a rat model of repeated concussion. J Neuroinflammation 10, 26.
30. Shultz, S.R., MacFabe, D.F., Foley, K.A., Taylor, R., and Cain, D.P. (2012). Sub-concussive brain injury in the Long-Evans rat induces acute neuroinflammation in the absence of behavioral impairments. Behav. Brain Res. 229, 145–152.
31. Rajan, R., Bourke, J., and Cassell, J. (2006). A novel stimulus system for applying tactile stimuli to the macrovibrissae in electrophysiological experiments. J. Neurosci. Methods 157, 103–117.
32. Rajan, R., Browning, A.S., and Bourke, J.L. (2007). Heterogeneity in the coding in rat barrel cortex of the velocity of protraction of the macrovibrissae. Eur. J. Neurosci. 25, 2383–2403.
33. Hartmann, M.J., Johnson, N.J., Towal, R.B., and Assad, C. (2003). Mechanical characteristics of rat vibrissae: resonant frequencies and damping in isolated whiskers and in the awake behaving animal. J. Neurosci. 23, 6510–6519.
34. Ritt, J.T., Andermann, M.L., and Moore, C.I. (2008). Embodied information processing: vibrissa mechanics and texture features shape micromotions in actively sensing rats. Neuron 57, 599–613.
35. Arabzadeh, E., Panzeri, S., and Diamond, M.E. (2004). Whisker vibration information carried by rat barrel cortex neurons. J. Neurosci. 24, 6011–6020.
36. Arabzadeh, E., Petersen, R.S., and Diamond, M.E. (2003). Encoding of whisker vibration by rat barrel cortex neurons: implications for texture discrimination. J. Neurosci. 23, 9146–9154.
37. Pinto, D.J., Brumberg, J.C., and Simons, D.J. (2000). Circuit dynamics and coding strategies in rodent somatosensory cortex. J. Neurophysiol. 83, 1158–1166.

38. Sanders, M.J., Dietrich, W.D., and Green, E.J. (2001). Behavioral, electrophysiological, and histopathological consequences of mild fluid-percussion injury in the rat. Brain Res. 904, 141–144.
39. Floyd, C.L., Golden, K.M., Black, R.T., Hamm, R.J., and Lyeth, B.G. (2002). Craniectomy position affects morris water maze performance and hippocampal cell loss after parasagittal fluid percussion. J. Neurotrauma 19, 303–316.
40. Levchakov, A., Linder-Ganz, E., Raghupathi, R., Margulies, S.S., and Gefen, A. (2006). Computational studies of strain exposures in neonate and mature rat brains during closed head impact. J. Neurotrauma 23, 1570–1580.
41. Lamy, M., Baumgartner, D., Yoganandan, N., Stemper, B.D., and Willinger, R. (2013). Experimentally validated three-dimensional finite element model of the rat for mild traumatic brain injury. Med. Biol. Eng. Comput. 51, 353–365.
42. Brands, D.W. *Predicting Brain Mechanics During Closed Head Impac—Numerical And Constitutive Aspects.* Ph.D. thesis, Technische Universiteit Eindhoven, (2002).
43. Mao, H., and Wagner, C. (2011). Material properties of adult rat skull. J. Mech. Med. Biol. 11, 1199–1212.
44. Gupta, R.K., and Przekwas, A. (2013). Mathematical models of blast-induced TBI: current status, challenges, and prospects. Front. Neurol. 4, 59.
45. Zhang, L., Yang, K.H., and King, A.I. (2004). A proposed injury threshold for mild traumatic brain injury. J. Biomech. Eng. 126, 226–236.
46. Ho, J., and Kleiven, S. (2009). Can sulci protect the brain from traumatic injury? J. Biomech. 42, 2074–2080.
47. Meyer, H.S., Schwarz, D., Wimmer, V.C., Schmitt, A.C., Kerr, J.N., Sakmann, B., and Helmstaedter, M. (2011). Inhibitory interneurons in a cortical column form hot zones of inhibition in layers 2 and 5A. Proc. Natl. Acad. Sci. U.S.A. 108, 16807–16812.
48. Weiss, J.H., Koh, J., Baimbridge, K.G., and Choi, D.W. (1990). Cortical neurons containing somatostatin- or parvalbumin-like immunoreactivity are atypically vulnerable to excitotoxic injury in vitro. Neurology 40, 1288–1292.
49. Petersen, C. C. (2009). in: *Encyclopedia of Neuroscience,* vol. 10. L. R. Squire (ed). Academic Press: pps. 41–45.
50. Griesemer, D., and Mautes, A. M. (2007). Closed head injury causes hyperexcitability in rat hippocampal CA1 but not in CA3 pyramidal cells. J. Neurotrauma 24, 1823–1832.
51. Yang, L., Afroz, S., Michelson, H.B., Goodman, J.H., Valsamis, H.A., and Ling, D.S. (2010). Spontaneous epileptiform activity in rat neocortex after controlled cortical impact injury. J. Neurotrauma 27, 1541–1548.
52. Akasu, T., Muraoka, N., and Hasuo, H. (2002). Hyperexcitability of hippocampal CA1 neurons after fluid percussion injury of the rat cerebral cortex. Neurosci. Letts. 329, 305–308.
53. Kao, T., Shumsky, J.S., Knudsen, E.B., Murray, M., and Moxon, K.A. (2011). Functional role of exercise-induced cortical organization of sensorimotor cortex after spinal transection. J. Neurophysiol. 106, 2662–2674.
54. Mulders, W.H., and Robertson, D. (2009). Hyperactivity in the auditory midbrain after acoustic trauma: dependence on cochlear activity. Neuroscience 164, 733–746.
55. Koralek, K.A., Jensen, K.F., and Killackey, H.P. (1988). Evidence for two complementary patterns of thalamic input to the rat somatosensory cortex. Brain. Res. 463, 346–351.
56. Brecht, M., and Sakmann, B. (2002). Dynamic representation of whisker deflection by synaptic potentials in spiny stellate and pyramidal cells in the barrels and septa of layer 4 rat somatosensory cortex. J. Physiol. 543, 49–70.
57. Lübke, J., Roth, A., Feldmeyer, D., and Sakmann, B. (2003). Morphometric analysis of the columnar innervation domain of neurons connecting layer 4 and layer 2/3 of juvenile rat barrel cortex. Cereb. Cortex 13, 1051–1063.
58. Nudo, R.J. (2013). Recovery after brain injury: mechanisms and principles. Front. Hum. Neurosci. 7, 887.
59. Charles, A., and Brennan, K. (2009). Cortical spreading depression—new insights and persistent questions. Cephalalgia 29, 1115–1124.
60. Basarsky, T.A., Duffy, S.N., Andrew, R.D., and MacVicar, B.A. (1998). Imaging spreading depression and associated intracellular calcium waves in brain slices. J. Neurosci. 18, 7189–7199.
61. Aitken, P.G., Tombaugh, G.C., Turner, D.A., and Somjen, G.G. (1998). Similar propagation of SD and hypoxic SD-like depolarization in rat hippocampus recorded optically and electrically. J. Neurophysiol. 80, 1514–1521.
62. Somjen, G.G. (2001). Mechanisms of spreading depression and hypoxic spreading depression-like depolarization. Phys. Rev. 81, 1065–1096.
63. Herreras, O., and Somjen, G.G. (1993). Propagation of spreading depression among dendrites and somata of the same cell population. Brain Res. 610, 276–282.
64. Theriot, J.J., Toga, A.W., Prakash, N., Ju, Y.S., and Brennan, K.C. (2012). Cortical sensory plasticity in a model of migraine with aura. J. Neurosci. 32, 15252–15261.
65. Rogatsky, G.G., Sonn, J., Kamenir, Y., Zarchin, N., and Mayevsky, A. (2003). Relationship between intracranial pressure and cortical spreading depression following fluid percussion brain injury in rats. J. Neurotrauma 20, 1315–1325.
66. Faden, A.I., Demediuk, P., Panter, S.S., and Vink, R. (1989). The role of excitatory amino acids and NMDA receptors in traumatic brain injury. Science 244, 798–800.
67. Katayama, Y., Becker, D.P., Tamura, T., and Hovda, D.A. (1990). Massive increases in extracellular potassium and the indiscriminate release of glutamate following concussive brain injury. J. Neurosurg. 73, 889–900.
68. Hayes, R.L., Jenkins, L.W., and Lyeth, B.G. (1992). Neurotransmitter-mediated mechanisms of traumatic brain injury: acetylcholine and excitatory amino acids. J. Neurotrauma 9, Suppl 1, S173–S187.
69. Nilsson, P., Gazelius, B., Carlson, H., and Hillered, L. (1996). Continuous measurement of changes in regional cerebral blood flow following cortical compression contusion trauma in the rat. J. Neurotrauma 13, 201–207.
70. von Baumgarten, L., Trabold, R., Thal, S., Back, T., and Plesnila, N. (2008). Role of cortical spreading depressions for secondary brain damage after traumatic brain injury in mice. J. Cereb. Blood Flow Metab. 28, 1353–1360.
71. Alder, J., Fujioka, W., Lifshitz, J., Crockett, D.P., and Thakker-Varia, S. (2011). Lateral fluid percussion: model of traumatic brain injury in mice. J. Vis. Exp. 54, 1–6.
72. Thompson, H.J., Lifshitz, J., Marklund, N., Grady, M.S., Graham, D.I., Hovda, D.A., and McIntosh, T.K. (2005). Lateral fluid percussion brain injury: a 15-year review and evaluation. J. Neurotrauma 22, 42–75.
73. Bolkvadze, T., and Pitkanen, A. (2012). Development of post-traumatic epilepsy after controlled cortical impact and lateral fluid-percussion-induced brain injury in the mouse. J. Neurotrauma 29, 789–812.
74. D'Ambrosio, R., Fairbanks, J.P., Fender, J.S., Born, D.E., Doyle, D.L., and Miller J.W. (2004). Post-traumatic epilepsy following fluid percussion injury in the rat. Brain 127, 304–314.
75. Englander, J., Bushnik, T., Duong, T.T., Cifu, D.X., Zafonte, R., Wright, J., Hughes, R., and Bergman, W. (2003). Analyzing risk factors for late posttraumatic seizures: a prospective, multicenter investigation. Arch. Phys. Med. Rehabil. 84, 365–373.
76. Alwis, D.S., and Rajan, R. (2013). Environmental enrichment causes a global potentiation of neuronal responses across stimulus complexity and lamina of sensory cortex. Front. Cell Neurosci. 7, 124.
77. Povlishock, J.T. (1993). Pathobiology of traumatically induced axonal injury in animals and man. Ann. Emerg. Med. 22, 980–986.
78. Povlishock, J.T., and Becker, D.P. (1985). Fate of reactive axonal swellings induced by head injury. Lab. Invest. 52, 540–552.
79. Povlishock, J.T., Becker, D.P., Cheng, C.L., and Vaughan, G.W. (1983). Axonal change in minor head injury. J. Neuropathol. Exp. Neurol. 42, 225–242.
80. Yaghmai, A., and Povlishock, J. (1992). Traumatically induced reactive change as visualized through the use of monoclonal antibodies targeted to neurofilament subunits. J. Neuropathol. Exp. Neurol. 51, 158–176.
81. McKee, A.C., Cantu, R.C., Nowinski, C.J., Hedley-Whyte, E.T., Gavett, B.E., Budson, A.E., Santini, V.E., Lee, H.S., Kubilus, C.A., Stern, R.A. (2009). Chronic traumatic encephalopathy in athletes: progressive tauopathy after repetitive head injury. J. Neuropathol. Exp. Neurol. 68, 709–735.
82. Fear, N.T., Jones, E., Groom, M., Greenberg, N., Hull, L., Hodgetts, T.J., Wessely, S. (2009). Symptoms of post-concussional syndrome are non-specifically related to mild traumatic brain injury in UK Armed Forces personnel on return from deployment in Iraq: an analysis of self-reported data. Psychol. Med. 39, 1379–1387.

83. Prins, M.L., Alexander, D., Giza, C.C., and Hovda, D.A. (2013). Repeated mild traumatic brain injury: mechanisms of cerebral vulnerability. J. Neurotrauma 30, 30–38.
84. Donovan, V., Bianchi, A., Hartman, R., Bhanu, B., Carson, M.J., and Obenaus, A. (2012). Computational analysis reveals increased blood deposition following repeated mild traumatic brain injury. NeuroImage Clin. 1, 18–28.
85. Leblanc, K.E. (1999). Concussion in sport: diagnosis, management, return to competition. Compr. Ther. 25, 39–45.

Address correspondence to:
Ramesh Rajan, PhD
Department of Physiology
Monash University
Wellington Road
Melbourne, Victoria 3800
Australia

E-mail: ramesh.rajan@monash.edu